# The Impacts of Unbalance on the Start-up Dynamics of Flexibly Mounted Rotors

Slavomír Jirků [1], Evžen Thöndel [2]
Technical University in Prague, Department of Electric Drives and Traction,
166 27 Praha 6, Czech Republic
[1] *jirku@fel.cvut.cz* , [2] *thoendee@fel.cvut.cz*

*Abstract* — **The paper deals with the impacts of unbalance on the start-up behaviour of flexibly mounted rotors with viscous damping. It provides an overview of the dimensionless parameters describing the system in question as well as the properties determining the influence of various degrees of static unbalance on the system start-up behaviour for different driving torque scenarios, such as transient-state and steady-state differences as opposed to balanced rotors, vibration-induced power losses, etc.**

*Keywords — Dynamics, unbalance, simulation, driving torque.*

## I. Mathematical Description of the System

The mechanical diagram of the system in question is provided in Fig. 1. Here, *m* stands for the rotor mass, $I_S$ the rotor moment of inertia with respect to the rotation axis, *e* the eccentricity defining the rotor static unbalance, *k* the stiffness of the flexible mounting, *B* the viscous damping constant and *M* the resulting external forces torque acting on the rotor; *x, y* are the coordinates of the rotation centre S with respect to the rest position 0 and φ the angle of the position vector going through the rotor centre of gravity T.

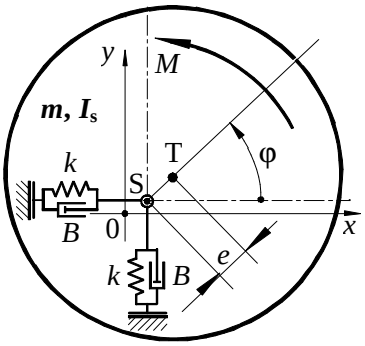


Fig. 1. Mechanical system diagram.

The equations of motion describing the system planar oscillations can be written as:

$$\begin{aligned} &\ddot{x} - e\ddot{\varphi}\sin\varphi = e\dot{\varphi}^2\cos\varphi - \omega_n^2 x - 2b\dot{x}\,, \\ &\ddot{y} + e\ddot{\varphi}\cos\varphi = e\dot{\varphi}^2\sin\varphi - \omega_n^2 y - 2b\dot{y} \\ &- me\ddot{x}\sin\varphi + me\ddot{y}\cos\varphi + I_S\ddot{\varphi} = M\,, \end{aligned} \tag{1}$$

where $\omega_n = \sqrt{k/m}$ is the angular eigen frequency of the system oscillations and $b = B/(2m)$ the relative damping factor. Dots above variables indicate their differentiation with respect to time.

To reduce the number of the system parameters, the following dimensionless (standardised) quantities can be introduced:

$$x^* = \frac{x}{i},\ y^* = \frac{y}{i},\ e^* = \frac{e}{i},\ \varphi^* = \varphi,\ t^* = \omega_n t\,,$$

$$M^* = \frac{M}{k\,i^2},\quad b^* = \frac{b}{\omega_n}, \tag{2}$$

where $i = \sqrt{I_S/m}$ is the radius of the rotor inertia. After substituting the above quantities into (1), the dimensionless forms of the equations can be written as:

$$\begin{aligned} &\ddot{x}^* - e^*\ddot{\varphi}^*\sin\varphi = e^*(\dot{\varphi}^*)^2\cos\varphi - x^* - 2b^*\dot{x}^*\,, \\ &\ddot{y}^* + e^*\ddot{\varphi}^*\cos\varphi = e^*(\dot{\varphi}^*)^2\sin\varphi - y^* - 2b^*\dot{y}^* \\ &- e^*\ddot{x}^*\sin\varphi + e^*\ddot{y}^*\cos\varphi + \ddot{\varphi}^* = M^*\,, \end{aligned} \tag{3}$$

where dots above dimensionless quantities indicate their differentiation with respect to the dimensionless time $t^*$.

## II. Excitation with a Linear Characteristic Torque

Let us now examine how the system behaves under the effects of a torque corresponding to an independent excited motor with $M_m = M_0 - B_m\omega$, $(\omega = \dot{\varphi})$ and the load torque $M_z = const.$ The resulting torque $M = M_m - M_z$ can be written in the dimensionless form

$$M^* = \frac{M_0 - M_z - B_m\omega}{k\,i^2} = M_0^* - M_z^* - b_m^*\omega^* \tag{4}$$

where $b_m^* = B_m/(I_S\,\omega_n)$ is the dimensionless motor parameter.

In case of a balanced rotor, the system does not oscillate and the time history of the rotor angular velocity can be analytically written as

$$\omega^*(t^*) = \omega_{0\infty}^*\left(1 - e^{-b_m^* t^*}\right) \tag{5}$$

where $\omega_{0\infty}^* = (M_0^* - M_z^*)/b_m^* = (M_0 - M_z)/(B_m\omega_n)$ is the dimensionless steady-state angular velocity for $e = 0$. As for unbalanced rotors $(e \neq 0)$, the non-linear system of equations was solved numerically using the Matlab software.

Figure 2 shows an example of the trajectories of the rotation centre S and of the rotor gravity centre T during

start-up with $e^* = 0.02$ and two different damping factor values of $b^* = 0.5$ and 2. The time history of the dimensionless angular velocity depends on other parameters, specifically $\omega^* = f(t^*, b^*, e^*, M_0^* - M_z^*, b_m^*)$.

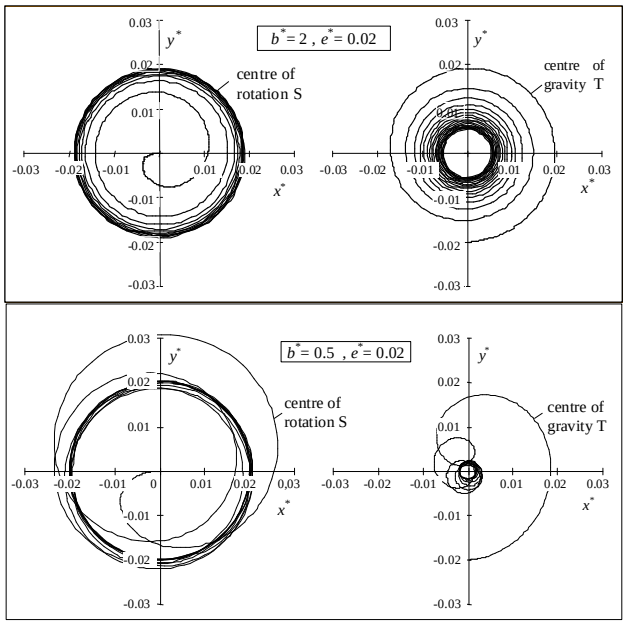


Fig. 2. Trajectories of the rotation centre S and the gravity centre T during rotor start-up.

However, after introducing the standardised quantities $\omega_{norm} = \omega^* / \omega_{0\infty}^* = \omega / \omega_{0\infty}$ (instantaneous angular velocity with respect to the steady-state value with $e = 0$) and $t_{norm} = t/\tau$, where $\tau = I_S / B_m$ is the start-up time constant, $\omega_{norm}$ will depend only on the parameters $t_{norm}$, $e^*$ and $b^*$, i.e. $\omega_{norm} = f(t_{norm}, e^*, b^*)$. Figure 3 shows this relationship for $b^* = 2$ and $e^* \langle 0; 0.06 \rangle$. It clearly demonstrates that in case of unbalanced rotor steady-state revolutions (marked as $\omega_{e\infty}$) decrease with increasing $e$.

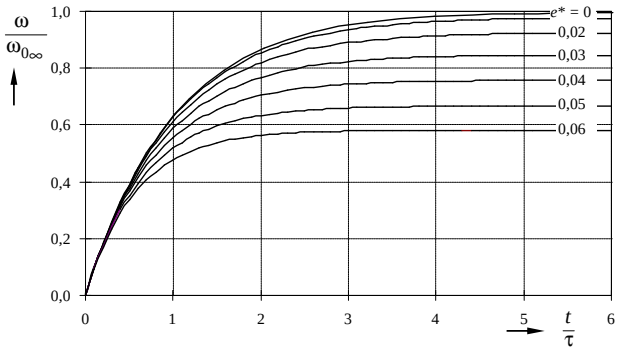


Fig. 3. Unbalanced rotor start-up.

Figure 4 shows the impacts of $e^* \langle 0; 0.1 \rangle$ and $b^* \langle 0; 10 \rangle$ on the $\omega_{e\infty} / \omega_{0\infty}$ ratio. The resulting decrease in revolutions and thus the power transferred to the load is caused by energy losses in the damper.

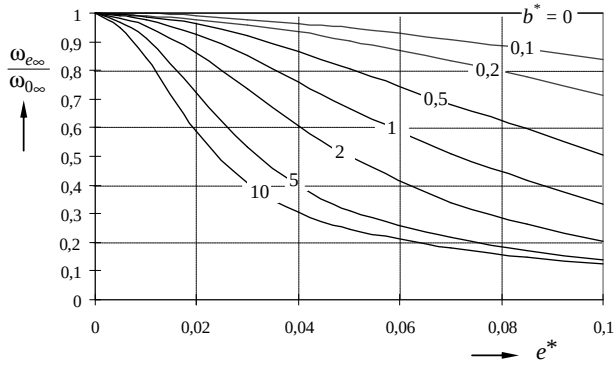


Fig. 4. Relation of steady-state revolutions to $e^*$ and $b^*$.

The power loss ratio can be written as

$$\delta(e^*, b^*) = \frac{M_z \omega_{0\infty} - M_z \omega_{e\infty}}{M_z \omega_{0\infty}} = 1 - \frac{\omega_{e\infty}}{\omega_{0\infty}}. \qquad (6)$$

The diagram for different values of $e^*$ and $b^*$, provided in Fig. 5 above, shows that extreme values can lead to significant losses of available power.

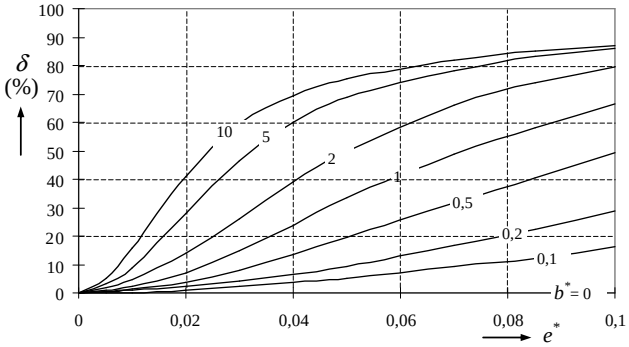


Fig. 5. The impact of $e^*$ and $b^*$ on energy losses.

## III. Excitation by a Non-Linear Torque with Induction Motor Characteristics

The following example shows how the system behaves when excited by a non-linear torque with the induction motor characteristics ( Kloss equation)

$$M_m = M_0 \frac{2\sigma s}{\sigma^2 + s^2}, \qquad (7)$$

where $s = 1 - \omega / \omega_{syn}$ is the slip in respect of the synchronous angular velocity $\omega_{syn}$, and $\sigma$ the parameter defining the slip value for which the torque has the maximum value of $M_0$. After substituting for $s$ the following formula can be obtained, showing how the torque relates to the angular velocity:

$$M_m = M_0 \frac{2\sigma \left(1 - \frac{\omega}{\omega_{syn}}\right)}{\sigma^2 + \left(1 - \frac{\omega}{\omega_{syn}}\right)^2}. \qquad (8)$$

Figure 6 shows the resulting curve for $\sigma = 0.25$, in which case the maximum is reached at $\omega_M = (1 - \sigma)\, \omega_{syn} = 0.75\, \omega_{syn}$.

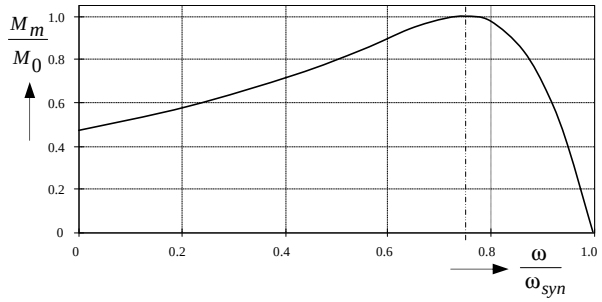


Fig. 6. Induction motor torque characteristic.

Similarly to the previous case, let us now introduce dimensionless variables according to equation (2) and assume a constant load torque $M_z$. The dimensionless form of the resulting torque can be written as:

$$M^* = \frac{M_m - M_z}{ki^2} = M_0^* \frac{2\sigma\left(1-\frac{\omega^*}{\omega_{syn}^*}\right)}{\sigma^2 + \left(1-\frac{\omega^*}{\omega_{syn}^*}\right)^2} - M_z^* \quad (9)$$

In case of a balanced rotor, the steady-state revolutions $\omega_{0\infty}$ can be calculated using the balance of the driving and load torques:

$$M_m = M_z \;\Rightarrow\; \omega_{0\infty} = \omega_{syn}\left[1-\sigma\left(\frac{M_0}{M_z} - \sqrt{\frac{M_0^2}{M_z^2}-1}\right)\right] \quad (10)$$

For instance for $\sigma = 0.25$ and $M_z = 0.4M_0$ equals to $\omega_{0\infty} = 0{,}948\,\omega_{syn}$. Considering the non-linearity of the equations, the time histories have to be calculated numerically. The results can again be generalised by introducing the standardised quantities

$$\omega_{norm} = \omega / \omega_{syn} \quad \text{and} \quad t_{norm} = t\,\omega_n^2 / \omega_{syn}.$$

In this case, the standardised angular velocity

$$\omega_{norm} = f(t_{norm}, b^*, M_0^*, M_z^*, \sigma).$$

Figure 7 shows the angular velocity time history during system start-up with

$$b^* = 2,\; M_0^* = 0.1,\; M_z^* = 0.4M_0^*,\; \sigma = 0.25.$$

The figure clearly shows that increasing unbalance results in a decrease of steady-state revolutions; after a certain value of $e^*$ is exceeded (in this case $e^* = 0.045$), the system steady state revolutions are lower than the value corresponding to the motor maximum torque, resulting in the motor running under unfavourable operating conditions.

Figure 8 shows the relation between an unstable rotor steady-state angular velocity $\omega_{e\infty}$ and the stable rotor velocity $\omega_{0\infty}$ for different values of $e^*$ with the given system parameters.

Similarly to the previous example, the loss of power transferred to the load can be defined according to equation (6).

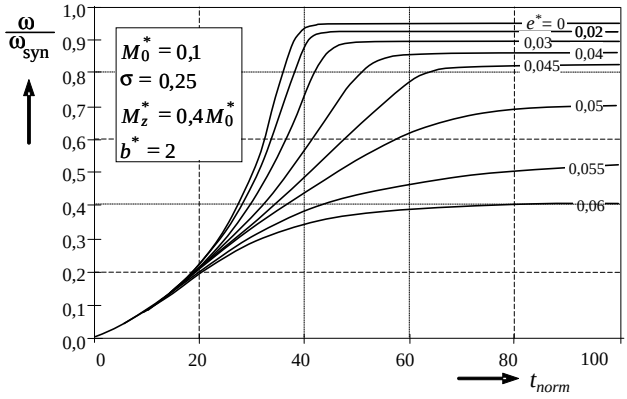


Fig. 7. Start-up of an unbalanced rotor.

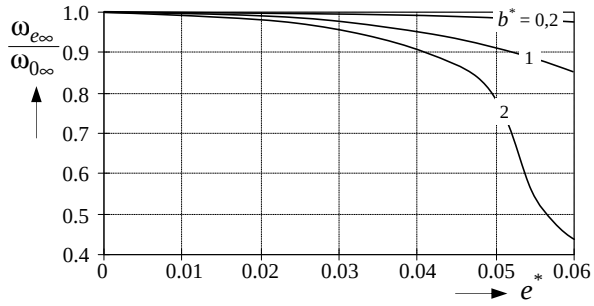


Fig. 8. The effects of $e^*$ and $b^*$ on steady-state revolutions.

The curves of the relative losses $\delta$ for different values of $e^*$ are provided in Fig. 9.

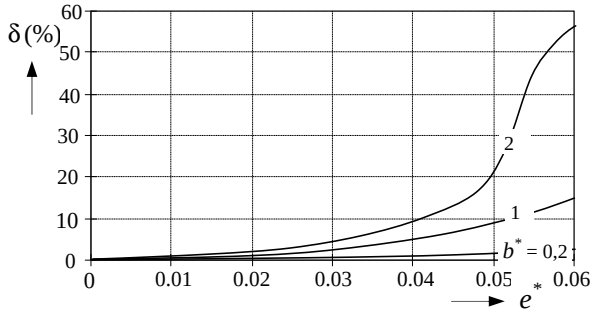


Fig. 9. The effects of $e^*$ and $b^*$ on performance losses.

## IV. CONCLUSION

The results presented in this paper show some of the potential issues of compensating the dynamical forces transferred by unbalanced rotors to the base by means of flexible mounts. Inertial forces acting upon an unbalanced rotor produce a torque opposite to the driving torque, resulting in a start-up and steady-state revolution decrease. This leads to losses of power transferred to the load, with energy being dissipated in the damper. However, calculations show that the effects of small imbalances are not too significant; the impacts of rotor unbalance are more pronounced only with higher eccentricity and damping factor values.

## REFERENCES

[1] A. Bedford and W. Fowler, *Engineering Mechanics – Statics & Dynamics*, Pearson Prentice Hall, Pearson Education Inc., New Jersey, 2005.

[2] J. Vondřich and S. Jirků, "Applications of Modeling of Machine Systems and Simulations of their Operating Behavior," *Proceedings of the Nineteenth IASTED International Conference Modeling, Identification and Control*, pp. 615-619, Innsbruck 2000.

[3] P. Kočárník and S. Jirků, "Simulation of Systems with Mechanical, Hydraulic and Thermodynamic Elements," in *Journal of Machine Engineering. Efficiency Development of Manufacturing Processes.* Vol. 6, No. 4, 2006. Editorial Institution of the Wroclaw Board of Scientific Technical Societies Federation NOT, Wroclaw, Poland. pp. 104-114. ISSN 1895-7595.

[4] J. Vondřich, E. Thöndel, and R. Havlíček, "Control of Machine Vibration with Absorber," in: *Journal of Machine Engineering. Efficiency Development of Manufacturing Processes.* Vol. 6, No. 3, 2006. Editorial Institution of the Wroclaw Board of Scientific Technical Societies Federation NOT, Wroclaw, Poland, pp. 72-79. ISSN 1895-7595.

[5] E. Thöndel, "Electric Motion Platform for Use in Simulation Technology – Design and Optimal Control of a Linear Electromechanical Actuator," in *Lecture Notes in Engineering and Computer Science.* Hong Kong: IAENG International Association of Engineers, 2010, pp. 960-965. ISBN 978-988-18210-0-3.

[6] J. Vondřich, J. and E. Thöndel, "Engineering Design of Machines with Rotating Members," in *Proceedings of the Eighth Latin American and Caribbean Conference for Engineering and Technology*, June 01–June 04, 2010 Arequipa, Peru [CD-ROM]. Lima: Pontificia Universidad Catolica, 2010, ISBN 0-9822896-3-4.

[7] J. Vondřich, J. and E. Thöndel, "Modeling Suppression of Non-linear Machine Vibration," *Journal of Machine Engineering*, 2010, Vol. 10, No. 2, pp. 45-50. ISSN 1895-7595.